J. Phys.: Condens. Matter **11** (1999) 7227–7242. Printed in the UK PII: S0953-8984(99)03508-0

The use of experimental data in constraining the tight-binding band parameters of quasi-two-dimensional organic molecular metals: application to α-(BEDT-TTF)$_2$KHg(SCN)$_4$

N Harrison†, E Rzepniewski‡, J Singleton‡, P J Gee‡, M M Honold‡, P Day§ and M Kurmoo§

† National High Magnetic Field Laboratory, LANL, MS-E536, Los Alamos, NM 87545, USA
‡ Department of Physics, University of Oxford, Clarendon Laboratory, Parks Road, Oxford OX1 3PU, UK
§ The Royal Institution, 21 Albemarle Street, London W1X 4BS, UK

Received 16 April 1999, in final form 22 July 1999

Abstract. Whilst tight-binding bandstructure calculations are very successful in describing the Fermi-surface configuration in many quasi-two-dimensional organic molecular metals, the detailed topology of the predicted Fermi surface often differs from that measured in experiments. This is very significant when, for example, the formation of a density-wave state depends critically on details of the nesting of Fermi-surface sheets. These differences between theory and experiment probably result from the limited accuracy to which the π-orbitals of the component molecules (which give rise to the transfer integrals of the tight-binding bandstructure) are known. In order to surmount this problem, we have derived a method whereby the transfer integrals within a tight-binding bandstructure model are adjusted until the detailed Fermi-surface topology is in good agreement with a wide variety of experimental data. The method is applied to the charge-transfer salt α-(BEDT-TTF)$_2$KHg(SCN)$_4$, the Fermi surface of which has been the source of much speculation in recent years. The Fermi surface obtained differs in detail from previous bandstructure calculation findings. In particular, the quasi-one-dimensional component of the Fermi surface is more strongly warped. This implies that upon nesting of these sheets, significant parts of the quasi-one-dimensional sheets remain, leading to a complicated Fermi-surface topology within the low-temperature, low-magnetic-field phase. In contrast to previous models of this phase, the model for the reconstructed Fermi surface in this work can explain virtually all of the current experimental observations in a consistent manner.

1. Introduction

The Fermi surfaces of quasi-two-dimensional organic molecular metals of the form α-(BEDT-TTF)$_2$MHg(SCN)$_4$ (where M = K, Tl or Rb) have been the subject of extensive experimental studies as a function of temperature and magnetic field [1]. At high temperatures and high magnetic fields, the Fermi-surface topology appears to be in broad agreement with calculations of the bandstructure made using the tight binding method [2]. Quantum oscillations of frequency $F_\alpha \approx 670$ T originate from a weakly warped quasi-two-dimensional cylinder of holes (the α-pocket), with the axis of this cylinder running parallel to the reciprocal-lattice vector $\boldsymbol{k}_b$. A second section of the Fermi surface consists of a pair quasi-one-dimensional electron sheets. At temperatures below $T_\mathrm{p} \sim 8$ K (M = K, Tl) or 10 K (M = Rb) and at magnetic fields below the 'kink' transition field at B_k ($B_\mathrm{k} \approx 23$ T (M = K), $\approx$25 T (M = Tl), or ≈ 32 T (M = Rb)) [3, 4], the Fermi surface takes on a modified form [3], generally thought

0953-8984/99/387227+16$30.00

to result from reconstruction through nesting of the quasi-one-dimensional sheets [5]. This is evidenced by the appearance of new quantum oscillation frequencies and a pronounced change in the behaviour of the angle-dependent magnetoresistance oscillations.

The nature of the low-temperature, low-field (LTLF) ground state is the subject of continuing debate. At fields far below B_k, the existence of an anisotropic magnetic susceptibility [6] and intrinsic magnetic moments [7] (revealed by muon-spin-rotation experiments) is suggestive of a spin-density-wave instability. On the other hand, the nearly isotropic nature of B_k and T_p with respect to the orientation of B appears to be suggestive of a Pauli-limiting mechanism [8, 9], which is a property more in common with charge-density-wave systems.

In this paper, we will not consider the details of the mechanism responsible for the LTLF states of these salts, but only the topology of the Fermi surface and its modification due to a translational nesting vector $\boldsymbol{Q}$. We shall concentrate on treating the M = K salt in detail, as the greatest amount of quantitative information is available for this compound. However, similar conclusions are expected to apply to the M = Tl and Rb salts and we shall make reference to relevant results for these materials (especially the M = Tl salt, which appears very similar to the M = K salt in many respects).

Two models have previously been proposed for the Fermi-surface topologies of the LTLF ground states of the α-(BEDT-TTF)$_2$MHg(SCN)$_4$ (M = K, Tl or Rb) salts [5, 10]. A common feature of these models is that the quasi-one-dimensional sheets are assumed to nest perfectly, therefore becoming dielectric. According to the model of Kartsovnik *et al* [5] (originally developed to explain Shubnikov–de Haas measurements made on the M = Tl salt), the $\boldsymbol{Q}$-vector causes the α-pockets to overlap in one direction giving rise to a new quasi-one-dimensional sheet, which is then consistent with angle-dependent magnetoresistance oscillation measurements within the LTLF state. The small lens-shaped pocket created by the intersection of the α-pockets is then proposed to account for a low frequency of $\sim$200 T observed in Shubnikov–de Haas oscillation measurements (or $\sim$180 T for the M = K salt) [11]; following common usage, we shall refer to this as the λ-frequency F_λ [11]. Another frequency $F_\nu \sim 860$ T (or 856 T for the M = K salt) [11] is proposed to correspond to the combination $F_\alpha + F_\lambda$, which is thought to occur as a result of magnetic breakdown [5]. More recent experimental investigations, however, have shown that while the ν-frequency is a pronounced feature in Shubnikov–de Haas measurements, it has an unusual temperature dependence and is completely absent from de Haas–van Alphen measurements [11]. The latter evidence suggests that the ν-frequency originates from quantum interference [11] rather than Landau quantum oscillatory effects. This observation, together with the observation of yet another frequency $F_\mu \approx 775$ T in both Shubnikov–de Haas and de Haas–van Alphen experiments, is incompatible with the reconstructed Fermi surface proposed by Kartsovnik *et al* [5]. More numerous Shubnikov–de Haas and de Haas–van Alphen frequencies are anticipated by the model of Uji *et al* [10], originally proposed to explain Shubnikov–de Haas measurements made on the M = Tl salt. This model is inadequate, however, because it is unable to account for the observation of quasi-one-dimensional sheets via angle-dependent magnetoresistance oscillations within the LTLF state [5, 12–17].

A likely reason for the failures of both of the above models to account for all of the experimental data is that they are based on the original unreconstructed Fermi surface calculated by Mori *et al* [2]. It is becoming increasingly apparent that while the calculation of Mori *et al* successfully predicts the essential elements (quasi-one-dimensional sheets and an α-pocket) of the Fermi surface, it is insufficient when we need to consider more detailed features of the topology [18]. Such details may have little influence on the behaviour of the salts within the high-magnetic-field, high-temperature phase, but can have profound consequences for the

degree of nesting and the topology of the Fermi surface within the LTLF phase. To emphasize this point, the M = NH_4 salt serves as a useful example; it is expected to have nearly the same Fermi surface as the M = K and Tl salts, yet does not revert to a spin-density-wave or charge-density-wave phase at low temperatures [19]. Instead it is found to be a superconductor with a critical temperature of $T_c \sim 1$ K.

Further deficiencies in the accuracy of the calculated Fermi surface become apparent when we consider the precise area and orientation of the α-pocket. The original Fermi-surface calculation for the M = K salt predicts this to occupy ∼19% of the Brillouin zone [2], whereas quantum oscillation studies have shown this to be ∼15.7% [1, 3–5, 10, 11, 18]. Angle-dependent magnetoresistance oscillation studies have also shown that this pocket is more elliptical than originally calculated [13–16], and that its major axis is tilted at an angle with respect to the reciprocal-lattice vector $\boldsymbol{k}_a$ [14, 16]. Bandstructure calculations have since been able to reproduce some aspects of the α-pocket topology more closely [20–23], but are still partially inaccurate in that they either wrongly estimate its area or underestimate the angle of tilt. While there have been extensive measurements made of the α-pocket, there have been no direct measurements made of the quasi-one-dimensional sheets of the unreconstructed Fermi surface, making comparisons between calculation and experiment more difficult in this case. A quantitative estimate of the gap between the α-pocket and the quasi-one-dimensional sheets has nevertheless been made through de Haas–van Alphen studies of the large magnetic breakdown frequency F_β [18]. The existence of this orbit, with an area in k-space equal to that of the Brillouin zone, requires electrons to tunnel between the quasi-one-dimensional and quasi-two-dimensional Fermi-surface sections. The size of the gap, determined by these measurements, is much smaller than that predicted by any of the bandstructure calculations [2, 20–23]. Thus there is mounting evidence to suggest that the current techniques used to calculate the band-structures of charge-transfer salts may not be capable of calculating their Fermi surfaces to the accuracy we desire. While the tight-binding method is probably the most reliable means for calculating their Fermi surfaces, this method is limited by the accuracy to which the π-orbitals of the BEDT-TTF molecules can be modelled. This is important because the transfer integrals are estimated from the degree of molecular overlap between the π-orbitals of neighbouring BEDT-TTF molecules.

Rather than calculating the transfer integrals from the molecular overlap determined theoretically, in this paper we adopt an alternative approach by which effective 'transfer integrals' t_i are fitted to the experimentally determined Fermi surface. In applying this method to α-(BEDT-TTF)$_2$KHg(SCN)$_4$, we assume only that the tight-binding Hamiltonian adequately describes charge transfer in this compound, and then adjust the t_i until a Fermi surface closely reproducing that determined experimentally is obtained. As a result of applying this procedure to α-(BEDT-TTF)$_2$KHg(SCN)$_4$, we find that the quasi-one-dimensional sheets of the calculated unreconstructed Fermi surface are more strongly warped than previously proposed, in agreement with the recent suggestion of Honold *et al* [18]. Consequently, there exists only one commensurate translational vector of the form $\boldsymbol{Q} = \frac{1}{5}\boldsymbol{k}_a + \zeta\boldsymbol{k}_b + \frac{2}{5}\boldsymbol{k}_c$, which is able to nest a significant portion of these sheets (where ζ represents an unknown interplane component). In contrast to the previous conjectures [5, 10], only ∼50% of the quasi-one-dimensional states become gapped by the order parameter. The incomplete nesting of the quasi-one-dimensional Fermi-surface sheets within the LTLF phase leads to a somewhat more complicated Fermi surface, but with all of the features necessary to explain both the experimentally observed angle-dependent magnetoresistance oscillation data within the LTLF phase, as well as the Shubnikov–de Haas and de Haas–van Alphen data. In particular, the ν-frequency is found to originate from quantum interference effects, as anticipated by House *et al* [11], and corresponds to an area in k-space equal to the area of the reconstructed Brillouin zone.

To verify the existence of further small Fermi-surface pockets anticipated by our model, we also report further measurements of the magnetoresistance within the LTLF phase. A low frequency of $\approx$113 T (close to the model prediction) is found to exist experimentally.

2. Fitting procedure

The process by which bandstructure parameters are adjusted in order to produce a Fermi surface that best represents the experimental data is a well-established technique for modelling the electronic structures of conventional three-dimensional metals [24]. This has typically involved a Korringa–Kohn–Rostoker (KKR) parametrization of the bandstructure whereby information on the Fermi-surface topology, obtained by angle-dependent de Haas–van Alphen measurements, is fed back into the calculation. Owing to the reduced dimensionality of quasi-two-dimensional organic metals, angle-dependent quantum oscillation measurements alone are not sufficient to extract all of the necessary information on the topology of their Fermi surfaces within the planes. Detailed information on the in-plane topology can only be obtained from angle-dependent magnetoresistance oscillation measurements. Since most of the gross geometrical properties of the Fermi surfaces of charge-transfer salts are predicted reliably by the tight-binding method (in which the bandstructure is described in terms of eight or so scalar transfer integrals) this provides a rather convenient means of parametrizing the Fermi surface. The fitting procedure is therefore considerably simpler than the Korringa–Kohn–Rostoker method; each of the 'transfer integrals' t_i in the tight-binding model can be adjusted in turn until a Fermi surface is obtained that is in satisfactory agreement with experiment. We emphasize at this point that the parameters t_i thus obtained are merely a convenient way of describing the Fermi surface; they should *not* be interpreted as the true transfer integrals that would be obtained in a rigorous calculation of the overlaps of the molecular π-orbitals. In a narrow-band metallic system such as a BEDT-TTF salt, the electrons will interact, almost certainly renormalizing the shape of the single-particle Fermi surface; the fitted t_i will include the effect of such interactions, whereas true transfer integrals would not.

Each time any one of the t_i is adjusted, the Fermi surface needs to be recalculated. Adopting the methods used for previous calculations of the bandstructures of α-phase salts [2], the four energy bands $\epsilon_j(\boldsymbol{k})$, that describe the transfer of electrons among the four inequivalent BEDT-TTF molecules, can be obtained by solving the secular equation

$$\langle\psi_1\cdots\psi_4|\boldsymbol{H}(t_1,\ldots,t_8)|\psi_1^*\cdots\psi_4^*\rangle = \langle\psi_1\cdots\psi_4|\epsilon(t_1,\ldots,t_8)|\psi_1^*\cdots\psi_4^*\rangle. \tag{1}$$

Here, the Hamiltonian is written in the form $\boldsymbol{H}(t_1,\ldots,t_8)$ in order to express the fact that it is dependent on the t_i which, in this case, are adjustable parameters. The solutions ϵ_j are therefore also unique to each set of parameters.

One way of assessing the quality of fit of the calculated Fermi surface to the experimental data is by comparing the shapes of various parts of the calculated Fermi surface with the results of fits to angle-dependent magnetoresistance oscillation data. For each Fermi-surface sheet j, this can be inferred from the size of the residual area ΔA_j which, in this context, is the net area in k-space enclosed between the perimeters of the calculated and experimental Fermi-surface components. Since the ultimate goal of this work is to obtain a fit to the entire Fermi surface, including all bands, the fitting procedure requires the sum of all residual areas $\sum_j \Delta A_j$ to be minimized.

It is convenient to represent the occupancy of filled electronic states for each band j by the Theta function

$$\rho_j(\boldsymbol{k}) = \Theta(\epsilon_j(\boldsymbol{k}) - \epsilon_F) \tag{2}$$

so that the total area of filled electron states in k-space for each band is given by the integral

$$A_j = \int\int \rho_j \, \mathrm{d}k_x \, \mathrm{d}k_y \, \cos\beta^*$$

over the Brillouin zone. Here, ϵ_F is the Fermi energy and $\beta^* \sim 90^\circ$ is the angle between the reciprocal-lattice vectors $\boldsymbol{k}_a$ and $\boldsymbol{k}_c$. The residual areas for each band can therefore be obtained via the integral

$$\Delta A_j = \int\int |\rho_j - \rho_{\mathrm{meas}}| \, \mathrm{d}k_x \, \mathrm{d}k_y \tag{3}$$

where ρ_{meas} represents the experimentally determined Fermi-surface component corresponding to that band.

Since the two lower-energy bands are completely filled, the residual areas for each of these bands is zero; hence $\Delta A_1 = \Delta A_2 = 0$. The third and fourth bands, however, intersect with the Fermi energy, the third giving rise to the α-pocket and the fourth giving rise to the quasi-one-dimensional sheets. Angle-dependent magnetoresistance oscillation experiments have shown that the shape of the α-pocket is indistinguishable from an ellipse with its major axis inclined at an angle θ with respect to $\boldsymbol{k}_a$. Using the elliptical approximation, the occupancy of filled electronic states is

$$\rho_{\mathrm{meas},\alpha} \approx \Theta\left(A_\alpha - \frac{\pi k_x'^2}{r} - \pi r k_z'^2 \right) \tag{4}$$

where A_α is the area of the α-pocket, determined most accurately by means of quantum oscillation experiments [1, 3–5, 10, 11, 18], and r is its ellipticity determined from angle-dependent magnetoresistance oscillation measurements [13–16]. To take account of the fact that the α-pockets are located at the corners of the Brillouin zone [2] and are inclined at an angle θ [14, 16], the k-vectors in equation (4) are modified by the translations

$$k_x' = (k_x \pm k_a/2)\cos\theta + (k_z \pm k_c/2)\sin\theta$$
$$k_z' = (k_z \pm k_c/2)\cos\theta - (k_x \pm k_a/2)\sin\theta.$$

ΔA_3 can then be found by substituting equation (4) into (3).

Since there have been no direct measurements of the topology of the quasi-one-dimensional sheets within the high-magnetic-field phase (or the high-temperature phase), it is not possible to make a precise estimate of the residual area ΔA_4 corresponding to the fourth band. Fortunately, because the topology of the Fermi surface is limited by certain constraints (which we list below), it is at least possible to make a first-order linear approximation relating ΔA_4 to the size of the gap in k-space $\Delta k_{x\ \mathrm{gap}}$ separating the quasi-one-dimensional sheets from the α-pocket. The first constraint is that the sum of the maximum extent of the α-pocket in the k_x-direction (which we shall label $k_{x\ \mathrm{max},\alpha}$) and the gap $\Delta k_{x\ \mathrm{gap}}$ defines at least one point in k-space on the quasi-one-dimensional (Q1D) Fermi surface. The k_x-component of this position vector is therefore $k_{x\ \mathrm{max,Q1D}} = k_{x\ \mathrm{max},\alpha} + \Delta k_{x\ \mathrm{gap}}$. The second constraint is that charge neutrality requires the area enclosed by the α-pocket and the area between the quasi-one-dimensional sheets to be equal. As a result of this latter constraint, any change $\delta k_{x\ \mathrm{max,Q1D}}$ in $k_{x\ \mathrm{max,Q1D}}$ must also involve a change $\delta(\Delta k_{\mathrm{warp}})$ in the amplitude of the warping Δk_{warp} of the quasi-one-dimensional sheets. At this point it is useful to consider a hypothetical model for the warping of the quasi-one-dimensional sheets of the form

$$k_x \simeq k_0 + (\Delta k_{\mathrm{warp}})\sin(2\pi k_z/k_c + \phi)$$

where ϕ is an arbitrary phase parameter [25]. If the maximum extent of the warping $|\Delta k_{\mathrm{warp}}|$ occurs in the vicinity of the gap, then according to this model, $\delta(\Delta k_{\mathrm{warp}})/\delta k_{x\ \mathrm{max,Q1D}} = -1$. Since $k_{x\ \mathrm{max},\alpha}$ is effectively fixed, then $\delta(\Delta k_{\mathrm{warp}})/\delta(\Delta k_{x\ \mathrm{gap}}) = -1$.

In the case of the quasi-one-dimensional sheets, the residual area is the area displaced by changing their degree of warping; hence

$$\partial(\Delta A_4)/\partial(\Delta k_{\mathrm{warp}}) \simeq \frac{2}{\pi}k_c$$

and therefore

$$\partial(\Delta A_4)/\partial(\Delta k_{x\ \mathrm{gap}}) \simeq -\frac{2}{\pi}k_c.$$

If $\Delta k_{x\ \mathrm{gap}}$ refers to the calculated gap and $\Delta k_{x\ \mathrm{meas}}$ refers to that obtained from magnetic breakdown measurements, then we can make the approximation

$$\Delta A_4 \sim \frac{2}{\pi}k_c|\Delta k_{x\ \mathrm{gap}} - \Delta k_{x\ \mathrm{meas}}|. \tag{5}$$

This can only be considered to be a rather approximate expression, since we ignore the higher harmonic components of the warping of the quasi-one-dimensional sheets [25]. Nevertheless, we succeed in combining all of the experimental factors (i.e. the area of the α-pocket, its ellipticity, its angle of inclination and the magnetic breakdown gap) into a single parameter ($\sum_j \Delta A_j$), which greatly simplifies the fitting procedure.

A rapid convergence of the fit is ensured by first making small adjustments $\pm\delta t_i$ to each of the t_i in order to estimate the first and second partial derivatives $\partial(\sum_j \Delta A_j)/\partial t_i$ and $\partial^2(\sum_j \Delta A_j)/\partial t_i^2$. In this way, an estimate of the change Δt_i in t_i required to minimize $\sum_j \Delta A_j$ (with respect to one t_i only) can be obtained by using the relation

$$\Delta t_i \sim -\left(\partial\left(\sum_j \Delta A_j\right)\Big/\partial t_i\right)\Big/\left(\partial^2\left(\sum_j \Delta A_j\right)\Big/\partial t_i^2\right).$$

An iteration is then complete once this procedure has been repeated for all i.

The original transfer integrals of Mori *et al* [2] provide a convenient point of departure from which to begin the fit; these are listed in table 1. This constrains our modified Fermi surface to be topologically similar to that of Mori *et al*; i.e. with the α-pockets located at the corners of the Brillouin zone and the quasi-one-dimensional sheets running through the centre of the Brillouin zone. Each of the eight t_i can be considered to represent a degree of freedom of the fit. Two of these are effectively lost by pinning the α-pocket to the V point of the Brillouin zone; i.e. a minimum of two t_i are required to define a closed pocket at this location. Another degree of freedom is lost by fixing the position of the quasi-one-dimensional electron states along the ΓZ axis; i.e. only one t_i is required to define a one-dimensional sheet if we do not consider its warping. One may further argue that charge neutrality imposes yet another

Table 1. A list of the t_i for α-(BEDT-TTF)$_2$KHg(SCN)$_4$ fitted to the Fermi surface in this work, and the corresponding transfer integrals of Mori *et al* and Campos *et al*.

Numeric label	Mori's label	t_{Mori} (meV)	t_{Campos} (meV)	t_{fit} (meV)
t_1	c_1	−19	7	−19.0
t_2	c_2	68	58	64.5
t_3	c_3	−11	29	−42.7
t_4	c_4	−14	—	−39.2
t_5	p_1	−100	54	−81.0
t_6	p_2	−97	58	−76.6
t_7	p_3	133	97	109.9
t_8	p_4	132	89	143.6

constraint, leaving effectively four degrees of freedom remaining for the fit. However, since the t_i are interdependent, one cannot associate any particular t_i with one particular feature of the Fermi surface.

3. Fitting results for α-(BEDT-TTF)$_2$KHg(SCN)$_4$

The accuracy of the fit is entirely dependent on the precision to which the Fermi surface of α-(BEDT-TTF)$_2$KHg(SCN)$_4$ has been measured by experiment. The area of the α-pocket is perhaps the most reliable information, with all of the more recent publications being unanimous in quoting $F_\alpha \sim 670$ T [1, 3–5, 10, 11, 18]. Values reported for its ellipticity r and inclination θ determined from angle-dependent magnetoresistance oscillation measurements are nevertheless more widely spread. Quasi-two-dimensional angle-dependent magnetoresistance oscillations providing information of the shape of the α-pocket have been performed at temperatures above T_p (at low magnetic fields) and at fields above B_k (at low temperatures) yielding similar results [13–16], and thereby indicating that the Fermi-surface topologies are essentially the same in the two regimes [16]. Similar results are also found under pressure at low magnetic fields and low temperatures [26]. Reported values of r range from 1.47 to 2.3, although the latter value was obtained from angle-dependent magnetoresistance oscillation measurements made at only a few azimuthal angles [15], in which it appears that the sample may have been misorientated [27]. More recent experiments by the same group support this assertion [16]. For the purpose of our fit, we shall take the average of the remaining values, giving $\bar{r} \sim 1.7 \pm 0.1$. With the exception of the experiments involving the misorientated sample [15,27] (in which θ is quoted as -58°), all angle-dependent magnetoresistance oscillation measurements [13, 14, 16, 26] indicate that θ is $\sim 15 \pm 3^\circ$.

Meanwhile, the estimate of the gap $\Delta k_{x\ \mathrm{meas}}$ in k-space between the α-pocket and quasi-one-dimensional sheets has only been obtained from a single measurement of the de Haas–van Alphen effect in strong magnetic fields, which yielded $\Delta k_{x\ \mathrm{meas}} \sim 4\%$ of $\boldsymbol{k}_a$ [18]. Since this gap is obtained from the logarithm of the ratio of the amplitudes of the de Haas–van Alphen β- and α-frequencies, the error in its determination is small.

The initial residual area $\sum_j \Delta A_j$ obtained by using the transfer integrals of Mori *et al* [2] prior to performing the fit occupies $\sim$12% of the Brillouin zone. After only four iterations, this is reduced to $\sim$0.5%. The fitted t_i are listed together with the transfer integrals [28] of Mori *et al* [2] and Campos *et al* [29] in table 1 [30]. The corresponding bandstructure and Fermi surface generated by the fit are shown in figures 1 and 2 respectively. It is immediately apparent from figure 2 that the fitted t_i are able to reproduce the experimental inclination of the α-pocket with respect to $\boldsymbol{k}_a$. This means that the α-pocket in figure 2 is considerably more inclined with respect to $\boldsymbol{k}_a$ than the predictions of previous bandstructure calculations [2, 20–23]. Furthermore, the gap between the sheets is smaller than in the *ab initio* calculations [2,20–23]; rather than having the form exactly of an ellipse, the reduction of the gap causes the α-pocket to develop into the shape of a 'rugby ball'. According to Mori *et al* [2] a reduced gap can potentially come about as a result of a reduction in the difference between the c_1-type and c_2-type transfer integrals. This is clearly not the case in the present calculations, as it is apparent in table 1 that these are relatively unaffected by the fit. This is due to the fact that the gap between the sheets no longer occurs at the Brillouin-zone boundary in our model. Meanwhile the increased inclination of the α-pocket can be attributed primarily to the large difference between the values of the p_2-type and p_4-type t_i. This difference is also responsible for the more strongly warped quasi-one-dimensional sheets [31].

On comparing the bandstructure calculation of figure 1 with that of Mori *et al* [2], it is apparent that while the overall electronic dispersion, consisting of four bands, has

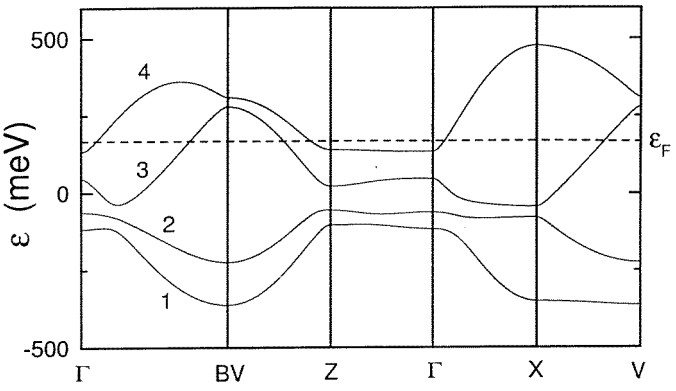

Figure 1. The bandstructure of α-(BEDT-TTF)$_2$(SCN)$_4$ after fitting the Fermi surface to that determined experimentally by means of quantum oscillations and angle-dependent magnetoresistance oscillation studies. The appropriate transfer integrals are listed in table 1. The various positions on the Brillouin zone can be inferred from figure 2. The bands are numbered as discussed in the text.

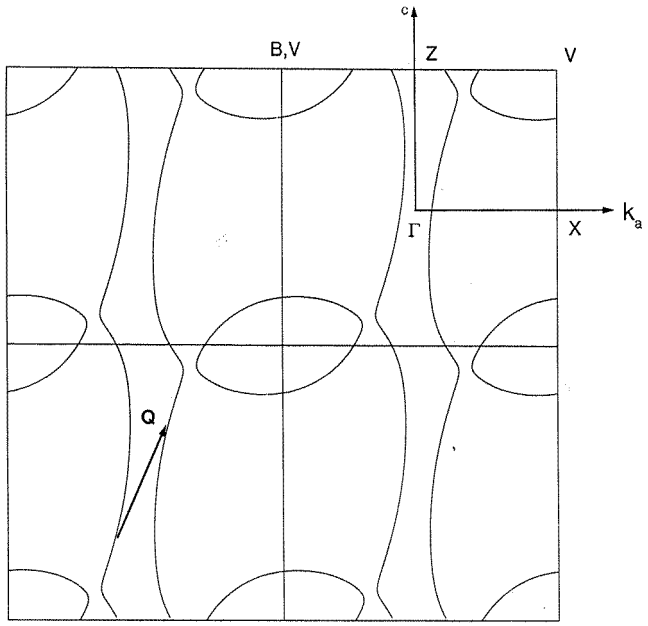

Figure 2. The Fermi surface corresponding to the bandstructure depicted in figure 1, in the extended-zone representation. The translational nesting vector $\boldsymbol{Q}$ is also depicted, as explained in the text.

approximately the same width, the individual bands have become slightly narrower and more widely separated. This is particularly true for the second-to-lowest band. A similar effect was noted in recent calculations of the bandstructure of κ-(BEDT-TTF)$_2$Cu(NCS)$_2$ as a result of incorporating the effects of the Coulomb repulsion U into the model [32]. While we have clearly not included U in the present calculation, the actual experimental Fermi surface is potentially modified by Coulomb effects; it is likely that the fitting of the t_i has attempted to take account of these modifications [28].

Finally, we remark that the fitted t_3 and t_4 differ by less than 10% (table 1). In this context, note that some workers have suggested that the corresponding transfer integrals (i.e. the input parameters to a single-electron bandstructure calculation) should be identical on symmetry grounds [21].

4. Fermi-surface nesting

One immediate result of the pronounced warping of the quasi-one-dimensional sheets in figure 2 is that it is no longer possible for these sheets to nest perfectly, as was assumed in previous models of the reconstructed Fermi surface of α-(BEDT-TTF)$_2$MHg(SCN)$_4$ [5, 10]. The more complicated form of the quasi-one-dimensional sheets in figure 2 also implies that there is only a limited range of $\boldsymbol{Q}$-vectors that can effectively nest a portion of these sheets (this contrasts with the Fermi-surface topology of Mori *et al* [2] in which the $\boldsymbol{k}_c$-component of the $\boldsymbol{Q}$-vector can assume almost any value); for example, there can only be one commensurate nesting vector, which is of the form $\boldsymbol{Q} = \frac{1}{5}\boldsymbol{k}_a + \zeta\boldsymbol{k}_b + \frac{2}{5}\boldsymbol{k}_c$, where ζ is an unknown interplane component. Any incommensurate nesting vectors must also be very close to this value, i.e. they will have to be of the form $\boldsymbol{Q} = (\frac{1}{5} + \delta_a)\boldsymbol{k}_a + \zeta\boldsymbol{k}_b + (\frac{2}{5} + \delta_c)\boldsymbol{k}_c$. In fact, detailed calculations [36] have been carried out for completely general nesting vectors, and it has been found that the energy of the system is minimized only when $\boldsymbol{Q} = \frac{1}{5}\boldsymbol{k}_a + \zeta\boldsymbol{k}_b + \frac{2}{5}\boldsymbol{k}_c$.

These nesting vectors depart somewhat from those suggested in previous works. Kovalev *et al* [14] proposed that $\boldsymbol{Q} = \frac{\zeta}{8}\boldsymbol{k}_a + \frac{3}{8}(\eta - \frac{1}{2})\boldsymbol{k}_b + \frac{3}{8}\boldsymbol{k}_c$ for the M = K salt while Kartsovnik *et al* [5] proposed that $\boldsymbol{Q} = \frac{\zeta}{6}\boldsymbol{k}_a + (\frac{\eta}{3} - \frac{1}{6})\boldsymbol{k}_b + \frac{1}{3}\boldsymbol{k}_c$ for the very similar M = Tl salt. These vectors were estimated from an analysis of the dependence of the periodicity of the quasi-one-dimensional angle-dependent magnetoresistance oscillations on the azimuthal angle within the LTLF phase. It would be a surprising fact if such notably different nesting vectors could exist in two salts with nearly the same Fermi-surface topology. More recent investigations of the quasi-one-dimensional angle-dependent magnetoresistance oscillations have shown that these nesting vectors may not have been as accurately determined as was originally thought. For example, while Kovalev *et al* [14] originally claimed that these quasi-one-dimensional sheets are inclined at an angle of $\varphi \sim 19^\circ$ with respect to $\boldsymbol{k}_c$, this value differs considerably from more recent φ-estimates which range as high as 30° [12, 13, 15–17].

Rather than corresponding to a sample-dependent nesting vector, it is more likely that this range of values originates from a spread in the uncertainty of the sample alignment. If we take the average of all these values we find that the mean angle is about $\bar{\varphi} \sim 24.3 \pm 2^\circ$. In the following section we will show that our proposed nesting vector gives rise to a quasi-one-dimensional sheet within the LTLF phase, in an analogous manner to the original model of Kartsovnik *et al* [5]. According to the $\boldsymbol{Q}$-vector determined in this work, the angle of inclination of the quasi-one-dimensional sheets is given by $\tan\varphi = Q_c/Q_a$, so $\varphi \sim 26.6^\circ$. This value is only approximately 2° larger than the angle obtained by averaging all of the experimental results and is well within the overall spread of values.

Like the previous nesting vectors that have been proposed, the vector components Q_a and Q_c obtained here are significantly less than the reciprocal-lattice vectors, resulting in a rather long periodicity for the spin or charge modulation. This situation is somewhat different to that for the simple $\boldsymbol{Q}$-vectors dealt with in standard spin-density-wave or charge-density-wave theories [33–35]. Furthermore, the spin-density-wave or charge-density-wave order nests only ∼50% of the quasi-one-dimensional states and therefore results in only a small change in the density of states at the chemical potential (Fermi energy). We can estimate the amount by which the electronic contribution to the density of states falls by considering the effective masses associated with the various parts of the Fermi surface. Quantum oscillation experiments have shown that the effective mass of the β-frequency is ∼3.5 m_e [18], where m_e is the free-electron mass. This large magnetic breakdown orbit encircles all of the states in k-space; its effective mass is therefore directly proportional to the total density of states of this salt. The effective masses of the α-pocket m_α and the quasi-one-dimensional (Q1D) sheets m_{Q1D} obey the sum relation $m_\alpha + m_{Q1D} = m_\beta$, and since $m_\alpha \sim 2\,m_e$, $m_{Q1D} \sim 1.5\,m_e$.

Thus, if ∼50% of the quasi-one-dimensional states become 'gapped' upon nesting (as will become clear in the following section), this leads to the removal of approximately 20% of the total electronic density of states through the establishment of the spin-density wave or charge-density wave. Because only ∼20% of the states at the Fermi surface can contribute to the spin or charge condensate within the LTLF phase, this may cause the spin or charge modulation to be rather weak, making it difficult to observe by diffraction techniques.

5. The reconstructed Fermi surface

The structure of the Fermi surface within the LTLF phase does not necessarily depend on whether this phase is a spin-density wave or a charge-density wave, but depends only on the $\boldsymbol{Q}$-vector and the magnitude of the order parameter. On applying the BCS-like expression $2\Delta_0 = 3.52k_{\mathrm{B}}T_{\mathrm{p}}$, we obtain an order parameter of ∼1.2 meV. However, since the effective mass m^* determined from experiment differs slightly from that obtained from the bandstructure calculation, m_{b}, the order parameter that we use to calculate the reconstructed Fermi surface needs to be renormalized. Our bandstructure calculation predicts that the mass of the β-orbit in α-(BEDT-TTF)$_2$KHg(SCN)$_4$ is ∼2.3 m_{e}, while experimentally it has been determined to be 3.5 m_{e} [11]. The effective order parameter Δ_{eff} that we use in the calculation should therefore be $\sim 1.5 \times \Delta_0$ which is ∼2 meV.

The reconstructed bandstructure is most easily computed in the case of a commensurate nesting vector. Choosing $\boldsymbol{Q} = \frac{1}{5}\boldsymbol{k}_a + \zeta\boldsymbol{k}_b + \frac{2}{5}\boldsymbol{k}_c$, the calculation of the reconstructed Fermi surface involves shifting the entire unreconstructed bandstructure by this vector fivefold, followed by the introduction of Δ_{eff} as a hybridization potential. For simplicity, we can assume Δ_{eff} to be isotropic and independent of energy. Theoretical models of spin-density-wave or charge-density-wave systems have typically involved a single band $\epsilon(\boldsymbol{k})$ shifted by a commensurate (or near commensurate) vector of the form $\boldsymbol{Q} = \boldsymbol{k}/2$ [33–35], which reduces to the effective hybridization of only two bands. Since the α-phase salts have four bands prior to nesting and the nesting vector is more complicated, this leads in the case of the M = K and Tl salts to the simultaneous hybridization of twenty bands. The modification of each of the bands $\epsilon'_{j'}$ by the order parameter can be obtained from the expression

$$\epsilon'_{j'} = \epsilon_{j'} + \sum_j \left(\sqrt{\left[\frac{\epsilon_j - \epsilon_{j'}}{2}\right]^2 + \Delta_{\mathrm{eff}}^2} - \left|\frac{\epsilon_j - \epsilon_{j'}}{2}\right| \right) \tag{6}$$

which is exact in the case of two bands. This of course assumes a mean-field order parameter Δ_{eff} which has the same value at all band crossings.

Figures 3 and 4 show the reconstructed bandstructure and Fermi surface respectively that result from this calculation. Note that this Fermi-surface model for the LTLF phase is considerably different from both that of Kartsovnik *et al* [5] and that of Uji *et al* [10]. Because the α-pockets (which are still recognizable in figure 5) are more elongated, they do not overlap. However, they do intersect with the residual pocket that remains as a result of the imperfect nesting of the quasi-one-dimensional sheets. This imperfect nesting results in an additional elongated hole pocket situated at the V′ point of the reconstructed Brillouin zone, with an initial area equivalent to a Landau quantum oscillation frequency of ∼180 T. This pocket is then truncated by intersection with the α-pocket, to leave an area corresponding to a frequency $\approx 125 \pm 20$ T. The large error results from the fact that the topology of this pocket, which we shall refer to as the γ-pocket, is very sensitive to uncertainties in the fitted unreconstructed Fermi surface.

The intersection of the α- and γ-pockets (which are both of the hole type) also gives

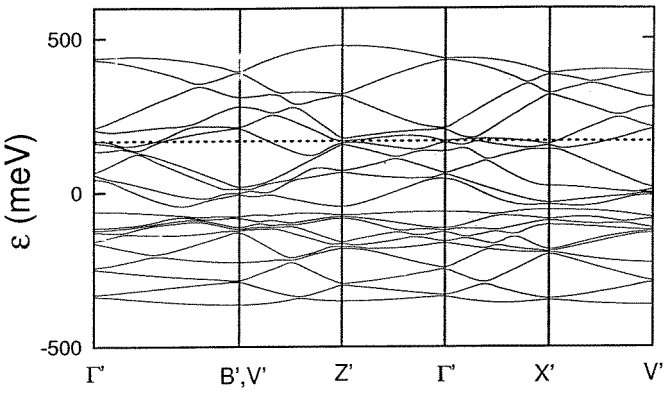

Figure 3. The reconstructed bandstructure calculated as described in the text. The positions within the reconstructed Brillouin zone are depicted in figure 4.

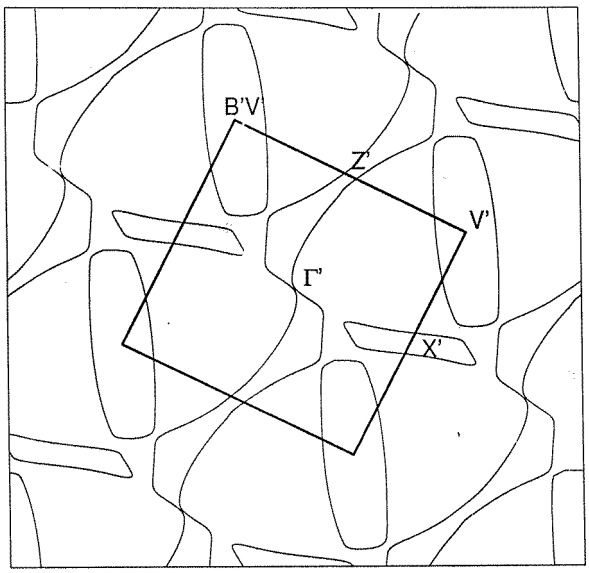

Figure 4. The reconstructed Fermi surface corresponding to the bandstructure shown in figure 3.

rise to the new set of quasi-one-dimensional sheets. These sheets lie along the $\Gamma'Z'$ axis of the reconstructed Brillouin zone which is rotated by an angle $\varphi \approx 26.6^\circ$ with respect to the original ΓZ axis as a result of the nesting vector. This angle is consistent with the results of angle-dependent magnetoresistance oscillation experiments within the LTLF phases of the M = K salt and the very similar M = Tl salt [5, 12–17]. The extra area residing between the α-pockets gives rise to an additional electron pocket situated at the X′ point of the reconstructed Brillouin zone, which is predicted to have an area of $\sim 39 \pm 20$ T.

The area of the reconstructed Brillouin zone is exactly five times smaller than that of the original Brillouin zone. Taking the value of the β-frequency observed by House *et al* [11], thought to correspond to the unreconstructed Brillouin-zone area, the reconstructed Brillouin zone is then found to correspond to a frequency of 854 T. This area agrees almost exactly with the ν-frequency F_ν ($\approx$856 T) observed in Shubnikov–de Haas measurements [5, 11], which was suggested by House *et al* [11] to result from quantum interference effects. A quantum interference frequency corresponding to an area in k-space equivalent to that of the Brillouin zone was recently found in two hexaboride compounds [37, 38] and was further proposed to

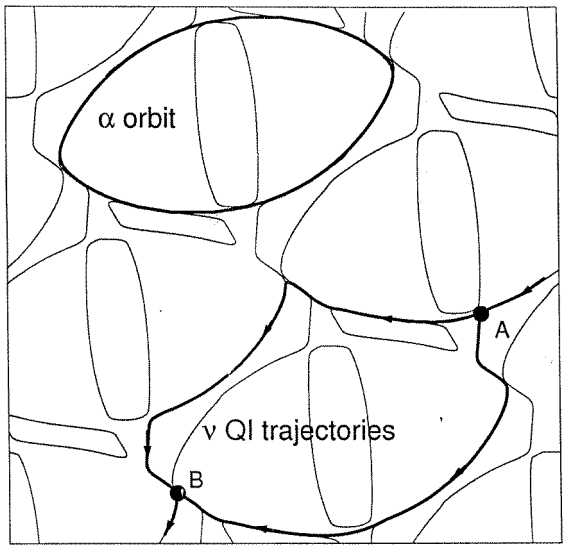

Figure 5. The quantum interference ν-trajectories which enclose an area in k-space equivalent to that of the reconstructed Brillouin zone. The α-pocket, which can be obtained through magnetic breakdown within the LTLF phase, is also shown.

occur in pure elemental Sn [37]. One conjecture that emerges as a result of studies of this effect in LaB_6 [37] is that Brillouin-zone quantum interference frequencies should occur in most two- or three-dimensional magnetic breakdown networks. One of the possible pairs of quantum interference trajectories enclosing an area equivalent to that of the new Brillouin zone is shown in figure 5. The letter A indicates the point at which the wave divides. The upper branch begins by following the path of part of one of the α-orbits, requiring magnetic breakdown across gaps opened up as a result of $\Delta_{\rm eff}$. The lower branch begins by following the quasi-one-dimensional sheets of the LTLF phase. This further requires magnetic breakdown to take place at the Γ point of the Brillouin zone, which is possible because of the small separation between the quasi-one-dimensional sheets at this point. The waves finally interfere at point B, with the phase enclosed between the two trajectories corresponding to a frequency of 854 T.

While we can explain the existence of the quantum interference ν-frequency, we cannot explain why it has an unusual temperature dependence [11], although we remark that, because its area is equivalent to that of the Brillouin zone, its associated effective mass is *zero* [37]. There now exist examples of quantum interference frequencies with unusual temperature dependences in several materials; examples include quantum interference in LaB_6 [37], and the 'rapid oscillations' in $TMTSF_2ClO_4$ which have been attributed to quantum interference [39].

A quantum interference trajectory corresponding to the λ-frequency ($\approx$183 T) of α-(BEDT-TTF)$_2$KHg(SCN)$_4$ can also be produced within our Fermi-surface model. In figure 5, this requires quasiparticles on the upper branch to make an additional excursion around one of the α-pockets. The quantum interference frequency is then given by the difference $F_\lambda = F_\nu - F_\alpha = 184$ T. Studies of the magnetoresistance of κ-(BEDT-TTF)$_2$Cu(NCS)$_2$ using both experimental data and numerical models [41] have shown that quantum interference frequencies often appear more strongly than do conventional Shubnikov–de Haas oscillations. This may explain why some of the other possible combination frequencies are relatively weak within the LTLF phase of α-(BEDT-TTF)$_2$KHg(SCN)$_4$ compared to the quantum interference orbits mentioned above.

The final prominent frequency observed within the LTLF phase (we shall examine some weak oscillations below) is the μ-frequency of $\approx$775 T [11]. The only way that a frequency of this order can occur in our model of the reconstructed Fermi surface is from the combination of

the α-frequency and that of the hole γ-pocket at V′. Thus, if $F_\mu = F_\alpha + F_\gamma$, then according to our model, $F_\mu \sim 795 \pm 20$ T. This is slightly larger than the frequency observed experimentally, although the difference could be accounted for by the uncertainty of the fit. In our model, F_μ is a conventional Landau quantum oscillation frequency, which explains why it is observable in both the Shubnikov–de Haas and de Haas–van Alphen effects [10, 11, 40]. The observation of the μ-frequency implies that F_γ should be observable at sufficiently low magnetic fields. According to our model, $F_\gamma \sim 125 \pm 20$ T, but if we take the experimental value of F_μ, this implies that $F_\gamma \sim 105$ T.

Figure 6(a) shows the results of additional low-magnetic-field, low-temperature experiments that were performed in order to study the possible existence of other quantum oscillatory features within the LTLF phase. A single crystal of α-(BEDT-TTF)$_2$KHg(SCN)$_4$ was measured within a dilution refrigerator using low-frequency, low-current lock-in techniques; the current was applied in the interplane direction. The Shubnikov–de Haas oscillations in figure 6(a) have been normalized by the background resistance. Fourier transformation of this signal reveals the usual frequencies within the LTLF phase (as shown in figure 6(b)), but also indicates the possibility of another frequency at ∼100 T. Only three periods of this frequency can exist within the interval of $1/B$ space in figure 6(b), so part of the information is lost by the application of a Hanning window; i.e. this effectively reduces the number of oscillations of this frequency to ∼1.5.

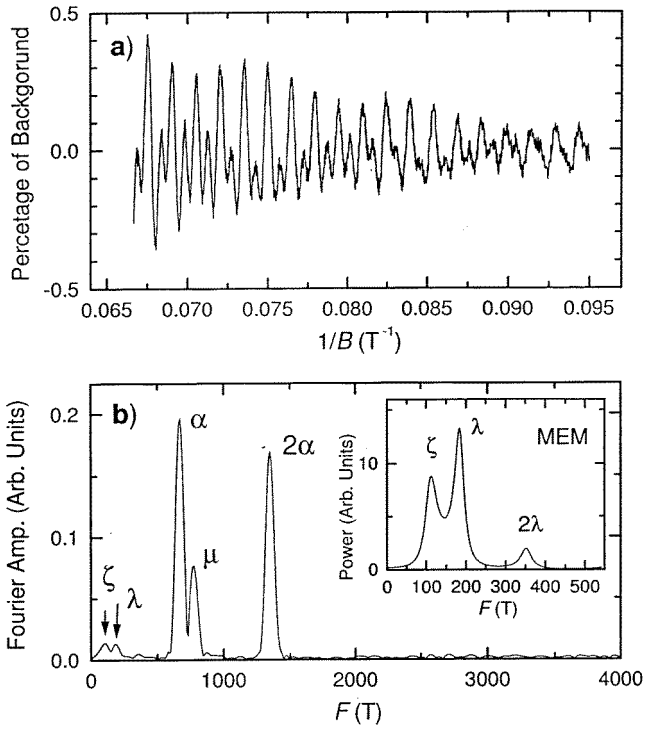

Figure 6. (a) Shubnikov–de Haas data for α-(BEDT-TTF)$_2$KHg(SCN)$_4$ taken at $T \sim 100$ mK, normalized by the background magnetoresistance. (b) Fourier transformation of the data shown in (a), with a power spectrum obtained by the MEM shown in the inset.

The maximum-entropy method provides an alternative means for analysing low-frequency oscillations. If we perform such a transform on the oscillations in figure 6(a) we obtain (at low frequencies) the maximum-entropy-method power spectral density in the inset to figure 6(b). The maximum-entropy method has the advantage of not requiring the application of a window function prior to performing the calculation, which therefore preserves more of the information.

The lowest of the frequencies in the inset to figure 6(b) is ∼113 T, and is therefore very close to the F_γ-frequency anticipated by our model. We can have confidence in the maximum-entropy method since it also produces sharper peaks for $F_\lambda \sim 183$ T as well as its harmonic $2F_\lambda$.

A comparison between the different M = K, Tl and Rb salts by Uji *et al* revealed that the frequencies which are common to two or more of these salts have very similar values [40]. We should therefore expect all of these salts to have Fermi-surface topologies that are nearly the same within the LTLF state. Since, according to Uji *et al*, there exist two low frequencies $F_\eta \sim 38$ T and $F_\kappa \sim 69$ T in the M = Tl salt, we should also expect similar frequencies in the M = K salt. It is possible that these frequencies may only have appeared in the M = Tl crystals because of their higher quality. On the other hand, both of these frequencies could conceivably be artefacts of the low-frequency noise [10]. However, the lower of these two frequencies is remarkably close to that expected for the electron pocket at the X′ point of the Brillouin zone. The higher frequency also could conceivably correspond to an additional $F_\kappa = F_\nu - F_\mu$ quantum interference frequency. More detailed studies of the LTLF phase are clearly required to address these questions.

Finally, we remark that there is no component of the Fermi surface in figure 4 with which the smaller pockets of Uji *et al* [10, 40] (referred to as δ and ϵ) can be immediately identified [42]. However, the calculations of the reconstructed Fermi surface in this work reveal that when the order parameter is reduced by ∼20%, further small pockets emerge close to the Γ point of the reconstructed Brillouin zone owing to the imperfect nesting of the quasi-one-dimensional sheets. This is a plausible explanation for the presence of the δ- and ϵ-frequencies in the work of Uji *et al* [10, 40].

A summary of the predicted and observed quantum oscillation frequencies is given in table 2.

Table 2. A list of the various frequencies observed in α-(BEDT-TTF)$_2$MHg(SCN)$_4$ salts within the LTLF phase, using the nomenclature described in the paper. Only the values of the frequencies measured, F_{meas}, in the M = K salt are shown, except for those frequencies that are observed only in the M = Tl salt. The third column shows the equivalent frequencies F_{model} to be expected from the reconstructed Fermi-surface model. The range of salts (i.e. M = K,Tl or Rb) in which the frequencies (or similar frequencies) are observed are listed in the fourth column. The fifth column addresses the origin of the oscillation, with LQ, MB and QI referring to Landau quantum oscillations, magnetic breakdown and quantum interference respectively; for magnetic breakdown or quantum interference combination frequencies, the means by which the combination is obtained is listed where necessary. The sixth column addresses the type of carrier enclosed by the pocket with e referring to electrons and h referring to holes. The final column refers to the location of the centre of the orbit within the reconstructed or unreconstructed Brillouin zone. Note that neither a carrier 'type' nor an orbit location can be assigned to the quantum interference frequencies.

F_{label}	F_{meas} (T)	F_{model} (T)	Seen in:	Origin	Type	Location
δ, ϵ	11	—	M = K, Tl	—	—	—
η	38	39	M = Tl	LQ	e	X′
κ	69	59	M = Tl	QI ($\nu - \mu$)	—	—
γ	113	125	M = K	LQ	h	V′
λ	183	184	M = K, Tl	QI ($\nu - \alpha$)	—	—
α	670	670	M = K, Tl, Rb	MB	h	V, V′
μ	775	795	M = K, Tl, Rb	MB ($\alpha + \gamma$)	h	V′
ν	856	854	M = K, Tl	QI (reconstructed Brillouin zone)	—	—
β	4270	4270	M = K, Tl, Rb	MB	h	Γ

6. Summary and conclusions

In this paper we describe a method for determining the topology of the Fermi surface of quasi-two-dimensional organic molecular metals by adjusting the parameters t_i of the tight-binding bandstructure so that it agrees with experimental data. We re-emphasize that the parameters t_i thus obtained are merely a convenient way of describing the Fermi surface; they should *not* be interpreted as the true transfer integrals that would be obtained in a rigorous calculation of the overlaps of the molecular π-orbitals. In a narrow-band metallic system such as a BEDT-TTF salt, the electrons will interact, almost certainly renormalizing the shape of the single-particle Fermi surface; the fitted t_i will include the effect of such interactions, whereas true transfer integrals would not.

On the application of this method to the charge-transfer salt α-(BEDT-TTF)$_2$KHg(SCN)$_4$, we obtain a Fermi-surface topology which is significantly different from the previous bandstructure calculation findings. The quasi-one-dimensional component of the Fermi surface is found to be more strongly warped, which implies that the nesting of these sheets is imperfect, giving rise to a different Fermi-surface topology within the LTLF phase. The model for the reconstructed Fermi surface in this work can explain the existence of canted quasi-one-dimensional sheets within the LTLF phase and the existence of quantum interference effects. One of the quantum interference frequencies (referred to as the ν-frequency) corresponds to an area in k-space equivalent to the area of the reconstructed Brillouin zone. Other observed Shubnikov–de Haas and de Haas–van Alphen frequencies are also in broad agreement with the Fermi-surface topology proposed in this work.

Acknowledgments

The calculations, which were carried out at Los Alamos National Laboratory, were supported by the Department of Energy, the National Science Foundation and the State of Florida. The experimental work, which was carried out at the Clarendon Laboratory, was supported by EPSRC (UK).

References

[1] For a recent review, see *Proc. Int. Conf. on the Science and Technology of Synthetic Metals (Snowbird, UT, 1996); Synth. Met.* 1997 **85+86**
[2] Mori H, Tanaka S, Oshima M, Saito G, Mori T, Maruyama Y and Inokuchi H 1990 *Bull. Chem. Soc. Japan* **63** 2183
[3] Pratt F L, Singleton J, Doporto M, Fisher A J, Janssen T J B M, Perenboom J A A J, Kurmoo M, Hayes W and Day P 1992 *Phys. Rev.* B **45** 13 904
[4] Osada T, Yagi R, Kawasumi A, Miura N, Oshima M and Saito G 1990 *Phys. Rev.* B **41** 5428
[5] Kartsovnik M V, Kovalev A E and Kushch N D 1993 *J. Physique* I **3** 1187
[6] Sasaki T, Sato H and Toyota N 1991 *Synth. Met.* **41–43** 2211
[7] Pratt F L, Sasaki T, Toyota N and Nagamine K 1995 *Phys. Rev. Lett.* **74** 3892
[8] Biskup N, Perenboom J A A J, Brooks J S and Qualls J S 1998 *Solid State Commun.* **107** 503
[9] Harrison N 1999 *Phys. Rev. Lett.* B **83** 1395
[10] Uji S, Terashima T, Aoki H, Brooks J S, Tokumoto M, Kinoshita N, Kinoshita T, Tanaka Y and Anzai H 1994 *J. Phys.: Condens. Matter* **6** L539
[11] House A A, Haworth C J, Caulfield J M, Blundell S J, Honold M M, Singleton J, Hayes W, Hayden S M, Meeson P, Springford M, Kurmoo M and Day P 1996 *J. Phys.: Condens. Matter* **8** 10 361
House A A, Haworth C J, Caulfield J M, Blundell S J, Honold M M, Singleton J, Hayes W, Hayden S M, Meeson P, Springford M, Kurmoo M and Day P 1996 *J. Phys.: Condens. Matter* **8** 10 371
[12] Iye Y, Yagi R, Hanasaki N, Kagoshima S, Mori H, Fujimoto H and Saito G 1994 *J. Phys. Soc. Japan* **63** 674
[13] Sasaki T and Toyota N 1994 *Phys. Rev.* B **49** 10 120

[14] Kovalev A E, Kartsovnik M V, Shibaeva R P, Rozenberg L P, Schegolev I F and Kushch N D 1994 *Solid State Commun.* **89** 575
[15] Caulfield J, Blundell S J, du Croo de Jongh M S L, Hendriks P T J, Singleton J, Doporto M, Pratt F L, House A, Perenboom J A A J, Hayes W, Kurmoo M and Day P 1995 *Phys. Rev.* B **51** 8325
[16] House A A, Blundell S J, Honold M M, Singleton J, Perenboom J A A J, Hayes W, Kurmoo M and Day P 1996 *J. Phys.: Condens. Matter* **8** 8829
[17] Lee I J, Naughton M J, Brooks J S, Valfells S, Uji S, Tokumoto M, Kinoshita N, Kinoshita T and Tanaka Y 1997 *Synth. Met.* **86** 2039
[18] Honold M M, Harrison N, Nam M-S, Singleton J, Mielke C H, Kurmoo M and Day P 1998 *Phys. Rev.* B **58** 7560
[19] Wang H H, Carlson K D, Geiser U, Kwok W K, Vashon M D, Thompson J E, Larsen N F, McCabe G D, Hulscher R S and Williams J M 1990 *Physica* C **166** 57
[20] Sasaki T, Ozawa H, Mori H, Tanaka S, Fukase T and Toyota N 1996 *J. Phys. Soc. Japan* **65** 213
[21] Rousseau R, Doublet M L, Canadell E, Shibaeva R P, Khasanov S S, Rozenberg L P, Kushch N D and Yagubskii E B 1996 *J. Physique* I **6** 1527
[22] Seo D-K, Whangbo M H, Fravel B and Montgomery L K 1996 *Solid State Commun.* **100** 191
[23] Ono S, Mori T, Endo S, Toyota N, Sasaki T, Watanube Y and Fukase T 1997 *Physica* C **290** 49
[24] Shoenberg D 1984 *Magnetic Oscillations in Metals* (Cambridge: Cambridge University Press)
[25] The sine expression is simply an algebraic tool that combines fitting the 'gap' between the Fermi-surface sheets and fitting the topology of the α-pocket in a single parameter; this enables us to estimate how to weight the importance of fitting the gap against other factors controlling the topology of the α-pocket. The inclusion of higher harmonics could perhaps improve this weighting process; however it would have only proved necessary to include higher harmonics if there had been a problem in finding a suitable set of t_i that optimized both the size of the gap and the α-pocket topology. In practice, it seems that the number of t_i is large enough for this not to be a concern.
[26] Hanasaki N, Kagoshima S, Miura N and Saito G 1997 *Synth. Met.* **86** 2025
[27] Caulfield J M 1997 private communication
[28] Again, we remark that our t_i are merely parameters which describe the observed Fermi-surface geometry (and which therefore include modifications of the Fermi surface due to many-body effects), whereas the transfer integrals of Mori *et al* [2] and Campos *et al* [29] are the input parameters of a single-electron bandstructure calculation inferred from the estimated overlaps of the BEDT-TTF molecular π-orbitals.
[29] Campos C E, Sandhu P S, Brooks J S and Ziman T 1996 *Phys. Rev.* B **53** 12 725
[30] It is difficult to give values for the errors on the various t_i in table 1. The *relative* sizes of the t_i are extremely well constrained by the input parameters which were used in the fit; shifts of $\sim\pm 0.2$ meV produced a noticeable degradation of the quality of fit. However, the *absolute* size of the parameters is controlled by the overall bandwidth, which is not well known (an order-of-magnitude estimate of the difference between predicted and experimental bandwidths can be gained by comparing predicted and experimental effective masses: see section 5).
[31] A similar conclusion, i.e. that the quasi-one-dimensional Fermi-surface sections in this salt should be more warped than those predicted by Mori *et al* [2], has been reached on purely theoretical grounds; see Gusmao G and Ziman T 1996 *Phys. Rev.* B **54** 16 663
[32] Demiralp E and Goddard W A III 1997 *Phys. Rev.* B **56** 11 907
[33] Kulikov N I and Tugushev V V 1984 *Usp. Fiz. Nauk* **144** 643 (Engl. Transl. 1984 *Sov. Phys.–Usp.* **27** 954)
[34] Grüner G 1988 *Rev. Mod. Phys.* **60** 1129
[35] Grüner G 1994 *Rev. Mod. Phys.* **66** 1
[36] Harrison N 1999 to be published
[37] Harrison N, Goodrich R G, Vuillemin J J, Fisk Z and Rickel D G 1998 *Phys. Rev. Lett.* **80** 4498
[38] Harrison N, Hall D W, Goodrich R G, Vuillemin J J and Fisk Z 1998 *Phys. Rev. Lett.* **81** 870
[39] Uji S, Terashima T, Aoki H, Brooks J S, Tokumoto M, Takasaki S, Yamada J and Anzai H 1996 *Phys. Rev.* B **53** 14 399
[40] Uji S, Terashima T, Aoki H, Brooks J S, Tokumoto M, Kinoshita N, Kinoshita T, Tanaka Y and Anzai H 1996 *Phys. Rev.* B **54** 9332
[41] Harrison N, Caulfield J, Singleton J, Reinders P H P, Herlach F, Hayes W, Kurmoo M and Day P 1996 *J. Phys.: Condens. Matter* **8** 5415
[42] Note that it is possible that δ and ϵ in fact correspond to a single frequency, which might be interpreted as two slightly different frequencies by the maximum-entropy method because of the limited range in field over which the frequency(ies) reside(s)